9-1987

A Turbulence Model for the Heat Transfer Near Stagnation Point of a Circular Cylinder

Mounir B. Ibrahim
Cleveland State University, m.ibrahim@csuohio.edu

Original Citation

Ibrahim, M., 1987, "A Turbulence Model for the Heat Transfer Near Stagnation Point of a Circular Cylinder," Applied Scientific Research, 44(3) pp. 287-302.

A turbulence model for the heat transfer near stagnation point of a circular cylinder

MOUNIR B. IBRAHIM
Mechanical Engineering Department, Fenn College of Engineering, Cleveland State University, Cleveland, OH 44115, USA

Abstract. A one-equation low-Reynolds number turbulence model has been applied successfully to the flow and heat transfer over a circular cylinder in turbulent cross flow. The turbulence length-scale was found to be equal $3.7y$ up to a distance 0.05δ and then constant equal to 0.185δ up to the edge of the boundary layer (where y is the distance from the surface and δ is the boundary layer thickness).

The model predictions for heat transfer coefficient, skin friction factor, velocity and kinetic energy profiles were in good agreement with the data. The model was applied for $\mathrm{Re} \leqslant 250{,}000$ and $\mathrm{Tu}_\infty \leqslant 0.07$.

Nomenclature

A_μ, C_D	Constants in the turbulence kinetic energy equation
C_1, C_2	Constants in the turbulence length-scale equation
C_{f_x}	Skin friction coefficient $\frac{\tau_w}{\frac{1}{2}\varrho u_\infty^2}$ at x.
D	Cylinder diameter
F	Dimensionless flow streamwise velocity u/u_e
k	Turbulence kinetic energy = 1/2 the sum of the squared three fluctuating velocities
K	Dimensionless turbulence kinetic energy k/u_e^2
I	Dimensionless temperature $(T - T_w)/(T_\infty - T_w)$
l	Turbulence length-scale
l_e	Turbulence length-scale at outer region
Nu_D	Nusselt number
p	Pressure
Pr	Prandtl number
Pr_t	Turbulent Prandtl number
Pr_k	Constant in the turbulence kinetic energy equation
R	Cylinder radius
Re_D	Reynolds number $\varrho_\infty u_\infty D/\mu_\infty$
Re_x	Reynolds number $\varrho_\infty u_\infty x/\mu_\infty$
R_K	Reynolds number of turbulence
T	Mean temperature
T_∞	Mean temperature at ambient
T_s	Mean temperature at surface
Tu_∞	Cross flow turbulence intensity, $\sqrt{u'^2}/u_\infty$
u	Mean flow streamwise velocity
u'	Fluctuating streamwise velocity
u_e	Mean flow velocity at far field distance
u_∞	Mean flow velocity at ambient
u^*	Friction velocity $= \sqrt{\tau_w/\varrho}$
v	Mean velocity normal to surface
V	Dimensionless mean velocity normal to surface
x, x_1	Distance along the surface

y	Distance normal to surface
β	Dimensionless pressure gradient parameter $= -\frac{x_1}{\varrho u_e^2}\left(\frac{dp}{dx_1}\right)$
δ	Boundary layer thickness at $u = 0.9995u_e$
η	Transformed coordinate in y direction
μ	Fluid molecular viscosity
μ_t	Turbulent viscosity
μ_{eff}	$\mu + \mu_t$
μ_∞	Fluid molecular viscosity at ambient
ν	Kinematic viscosity μ/ϱ
ϱ	Density
ϱ_∞	Density at ambient
τ_w	Wall shear stress
$\tau_{w,0}$	Wall shear stress at zero free stream turbulence

1. Introduction

Recently, considerable attention [1–3] has been given to study the fluid flow and heat transfer characteristics near the forward stagnation point of a circular cylinder in turbulent cross flow. The most related engineering application to this study is the forward stagnation point of a gas turbine blade. With the recent high operational gas temperature, the knowledge of the heat transfer at the leading edge becomes vital to the turbine blade cooling design. Experiments on circular cylinders [4] indicate increases in the heat transfer coefficient and the skin friction factor (compared to the corresponding laminar flow values) by 70% and 50% respectively, for Reynolds number (Re_D) 24,000 and free stream turbulence intensity (Tu_∞) 6%.

The challenges provided by the above phenomena attracted many research workers [3–8] to conduct heat transfer experiments for circular cylinder placed in turbulent cross flow. Indespite of the scatter found in the measured Nusselt number (Nu_D) for different Re_D and Tu_∞, all data confirmed the considerable increase in the heat transfer coefficient due to the free stream turbulence as indicated above.

On the other hand, several theoretical models were proposed in the literature to study the above phenomena, those models include zero-equation, two-equation and multi-equation turbulence models.

Zero-equation turbulence model was introduced by Smith and Kuethe [4] assuming the eddy viscosity to be proportional to the turbulence in the free stream. The proportionality constant have been determined from the experimental data. Miyazaki and Sparrow [9] applied an eddy diffusivity formulation using as a basis the empirical formula of Belov et al. [10]. The eddy diffusivity was assumed proportional to the turbulence in the free stream and a mixing length similar to that used in boundary layer analysis for flat plates. Also, the model included a constant that was determined by matching the experimental data. Kwon et al. [1] used the model proposed by Miyazaki and Sparrow with a new version to include an explicit pressure

gradient dependency. It should be noted that in the above models, a constant turbulent Prandtl number was used. Also, the predictions were only compared with experimental data for $Nu_D\ Re_D^{-1/2}$ versus $Tu_\infty\ Re_D^{1/2}$.

Two-equation models have also been applied to study the above phenomena [3, 11]. However, a third equation was introduced by Hijikata et al. [3] to account for the anisotropic turbulence effects. This implied the inadequacy in the ε-equation as a length scale determining equation; this implication was also reported by Patel et al. [12] for some other engineering applications.

Most recently, Wang [2] applied a Reynolds-stress turbulence model to analyze the turbulence characteristics for the above phenomena. However, in order to close the modeling, it was necessary to assume a turbulence length-scale as an empirical input. The selected length-scale was a modified form from the one used in boundary layer flat plate flow, in order to match the predicted Nu_D with the available experimental data. Also Wang used a large temperature difference (55°C) between the cylinder surface and the free stream temperatures. This large temperature difference might have contributed to an effect of the physical property variations in the predicted Nu_D. With regard to applying Reynolds-stress turbulence model, some discrepancies were reported recently, between the predicted and the measured turbulent quantities in some other engineering applications [13–15]. Those discrepancies were attributed, partly, to some shortcoming in the Reynolds-stress model.

The above review of the literature emphasized the fact that for the present type of problems, it is necessary to assume a turbulence length-scale or introduce modifications for the length-scale determining function. In the present work, an attempt is made to use a one-equation turbulence model with a low-Reynolds number version [16]. A simple turbulence length-scale is proposed, its form to be determined by matching the predictions with available data for heat transfer coefficient, skin friction factor, velocity profiles and turbulent kinetic energy profiles. Reported herein is the numerical procedure used in this study. The governing equations are introduced, then the turbulence model is discussed. A computational scheme is developed to simulate the existing experiments. The computational results are then discussed and compared with the available experimental data for the fluid flow and heat transfer characteristics.

2. Governing equations

The flow is assumed to be two-dimensional, steady and incompressible turbulent boundary layer with constant physical properties. The governing equations were first written in a curviliner coordinate system (x, y domain),

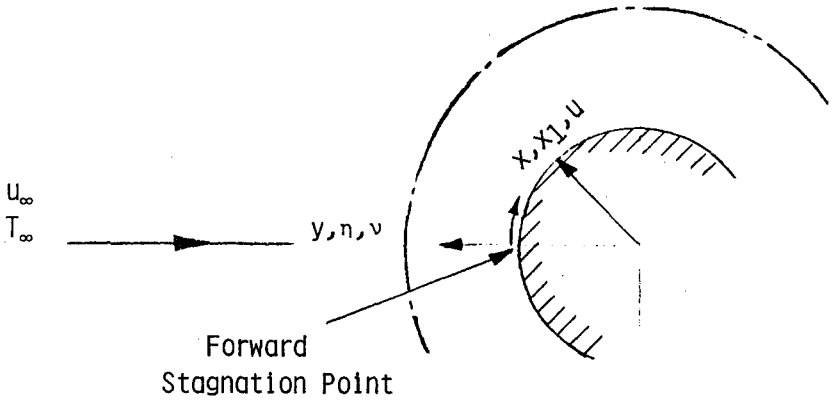

Fig. 1. Sketch of the coordinate systems used in this study (x, y) and (x_1, η).

then transformed to a convenient form using the transformation described below.

For the present analysis, the boundary layer thickness is assumed to be small in comparison to the cylinder radius. Also, the computation is confined to a distance (x) very close to the forward stagnation point $(x \simeq 0)$. Using the transformation:

$$x_1 = x, \quad \eta = y(\varrho_\infty u_e/\mu_\infty x_1)^{1/2}, \quad F = u/u_e,$$

$$V = v(\varrho_\infty x_1/\mu_\infty u_e)^{1/2} + x_1 F \frac{\partial \eta}{\partial x} \quad \text{and} \quad I = \frac{T - Tw}{T_\infty - Tw}.$$

Figure 1 is a sketch for the two coordinate systems. Now the basic governing equations (continuity, momentum and energy) take the forms:

Continuity

$$x_1 \frac{\partial F}{\partial x_1} + \frac{\partial V}{\partial \eta} + \frac{F}{2}(\beta + 1) = 0 \tag{1}$$

Momentum

$$x_1 F \frac{\partial F}{\partial x_1} + F^2 \beta + V \frac{\partial F}{\partial \eta} = \beta + \frac{\partial}{\partial \eta}\left[\frac{\mu_{\text{eff}}}{\mu_\infty}\left(\frac{\partial F}{\partial \eta}\right)\right] \tag{2}$$

Energy

$$x_1 F \frac{\partial I}{\partial x_1} + V \frac{\partial I}{\partial \eta} = \frac{\partial}{\partial \eta}\left[\left(\frac{1}{\mathrm{Pr}} + \frac{\mu_t/\mu_\infty}{\mathrm{Pr}_t}\right)\frac{\partial I}{\partial \eta}\right] \tag{3}$$

where

$$\mu_{\mathrm{eff}} = \mu + \mu_t, \quad \beta = -\frac{x_1}{\varrho u_e^2}\left(\frac{\mathrm{d}p}{\mathrm{d}x_1}\right) = \frac{x_1}{u_e}\frac{\mathrm{d}u_e}{\mathrm{d}x_1}.$$

A potential flow fluid was assumed at the external far field, therefore:

$$u_e = 4u_\infty x_1/D \tag{4}$$

Equations 1–3 are subjected to the following boundary conditions:

$$\begin{aligned} &F(x_1, 0) = V(x_1, 0) = I(x_1, 0) = 0 \\ &F(x_1) \to 1 \quad \text{and} \quad I(x_1) \to 1 \text{ as } \eta \to \infty. \end{aligned} \tag{5}$$

3. Turbulence modeling

For negligible free stream turbulence intensity, a thin laminar boundary layer is developed in the vicinity of the forward stagnation point of a cylinder in cross flow. As the free stream turbulence intensity increases the boundary layer becomes thicker and of a turbulent nature. Therefore, in analyzing the effect of free stream turbulence on the fluid flow and heat transfer characteristics, a low-Reynolds-number turbulence model should be utilized. In the present study, the following transport equation for the turbulence kinetic energy was assumed, which is similar in form to that used by Hassid and Poreh [16] and El-Hadidy [17]:

$$\varrho u \frac{\partial k}{\partial x} + \varrho v \frac{\partial k}{\partial y} = \frac{\partial}{\partial y}\left[\left(\mu + \frac{u_t}{\mathrm{Pr}_k}\right)\frac{\partial k}{\partial y}\right] + \mu_t\left(\frac{\partial u}{\partial y}\right)^2 - \left[\frac{2\nu k}{l^2} + \frac{C_D k^{3/2}}{l}(1 - \exp(-A_\mu \mathrm{R}_k))\right] \tag{6}$$

with the boundary conditions

$$k(x, 0) = 0 \quad k(x, \delta) = k(\delta). \tag{7}$$

The turbulent viscosity μ_t was related to the turbulence kinetic energy by the Prandtl–Kolmogorov formulation with a damping function:

$$\mu_t = C_D^{1/3} k^{1/2} l\varrho[1 - \exp(-A_\mu \mathrm{R}_k)]. \tag{8}$$

In the above equations 6–8, Pr_k, A_μ and C_D are constants and equal to 1.0, 0.03 and 0.164 respectively. Those constants are obtained from matching predictions with experimental data for a good number of engineering applications. Also, l is the turbulence length-scale and R_k is the Reynolds number of turbulence:

$$\mathrm{R}_k = \frac{l\varrho k^{1/2}}{\mu}. \tag{9}$$

Using the previous transformation together with $K = k/u_e^2$, equations 6–9 take the following formats:

$$x_1 F \frac{\partial K}{\partial x_1} + 2FK\beta + V\frac{\partial K}{\partial \eta} = \frac{\partial}{\partial \eta}\left[\left(\frac{\mu + \mu_t/\mathrm{Pr}_k}{\mu_\infty}\right)\frac{\partial K}{\partial \eta}\right] + \left(\frac{\mu_t}{\mu_\infty}\right)\left(\frac{\partial F}{\partial \eta}\right)^2$$

$$- \left[2k\left(\frac{x_1}{l}\right)\frac{\mu}{\varrho u_e l} + C_D k^{3/2}\left(\frac{x_1}{l}\right)(1 - \exp(-A_\mu \mathrm{R}_k))\right]. \tag{10}$$

Boundary conditions

$$\begin{aligned} K(x_1, 0) &= 0 \\ K(x, \delta) &= K(\delta) \end{aligned} \tag{11}$$

$$\mu_t/\mu = C_D^{1/3}\mathrm{R}_k[1 - \exp(-A_\mu \mathrm{R}_k)] \tag{12}$$

and

$$\mathrm{R}_K = \frac{\varrho u_e l}{\mu} K^{1/2}. \tag{13}$$

A constant value of the turbulent Prandtl number (Pr_t) has been used across the boundary layer = 0.9.

4. Numerical method

Upon describing the turbulence length-scale (l) and for a given pressure gradient parameter (β) and external flow conditions, equations 1–5 and 10–13 conform a closed system to be used for solving the boundary layer external flow. An implicit finite difference scheme has been utilized which computes the entire viscous flow from the wall outward. The resulting system of algebraic equations was solved using the Thomas algorithm [18]. The finite difference scheme used in this study is similar to that used by Pletcher [19].

A variable grid size in the η direction was used with $\Delta\eta = 0.005$ at the wall and increases by a factor 1.03 when moving away from the wall; this resulted in using 125–165 grid points. Also, an interative procedure has been used with the following convergence criterion:

$$|\phi_j^N - \phi_j^{N-1}|/\phi_j^N \leqslant 0.0001$$

where ϕ_j^N is the value of ϕ at the jth grid node after Nth interation cycle and ϕ_j^{N-1}, that for the $(N-1)$th interation cycle. The number of interations did not exceed 10 in any of the cases studied, and the computer time was about 0.326 seconds on UNIVAC 1100/80 for each single run.

5. Turbulence length-scale

Hassid and Poreh [16] and El-Hadidy [17], in using the above turbulence model, employed Nikuradse [20] turbulence length-scale for a pipe flow. Their predictions for the fluid flow and heat transfer were in good agreement with the available experimental data.

In the present study, it was found necessary to test the model for its predictions in the simple case of flat plate with zero pressure gradient. A standard form of the turbulence length-scale (l) have been used:

$$\begin{aligned} l &= 0.4y \qquad 0 < y < 0.225\delta \\ l_e &= 0.09 \qquad 0.225\delta < y < \delta. \end{aligned} \tag{15}$$

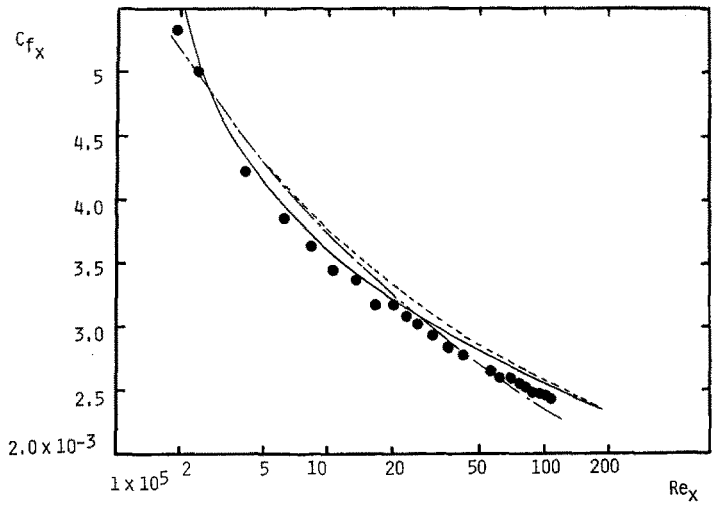

Fig. 2. Skin friction on a smooth flat plate for present work as compared with data —— Present work, ● Experimental data [22], – – – $C_{fx} = 0.455/\ln^2(0.06\,\mathrm{Re}_x)$ [23], – · – $C_{fx} = 0.0592\,\mathrm{Re}_x^{-0.2}$ [23].

The calculation was started at $\mathrm{Re}_x = 10^5$ with input values of F and V from exact numerical solutions to laminar Blasius flow. The input profile for the turbulence kinetic energy was similar to that used by Beckwith and Bushnell [21]. For this particular case, the grid size in x_1 direction (Δx_1) was taken as 2.0δ.

Figure 2 shows the predictions of C_{fx} vs. Re_x for a flat plate with zero pressure gradient using the above model. The predictions are compared with some experimental data (22) and empirical correlations (23); the agreement is good. Figure 3a shows the predictions of k/u^{*2} vs. yu^*/ν in the near wall region and compared with the theoretical model of Jones and Launder [24] and the experimental data of Kreplin and Eckelmann [25]. The present model is showing little improvement to Jones and Launder model as compared with the data. The predictions of k/u^{*2} away from the wall are given in Fig. 3b and are in agreement with the measurements of Klebanoff given in Hinze [26].

From the above test case, it was concluded that the proposed model is predicting the data reasonably well for the simple flat plate case with zero pressure gradient.

In extending the proposed turbulence model to the flow field in the vicinity of the stagnation point, two changes should be considered. First, the damping function used in formulating the turbulent viscosity (equation 12) should be excluded. This is similar to the approach used for zero-equation

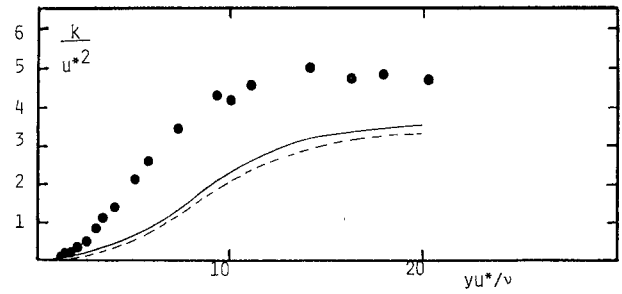

Fig. 3a. Measured and calculated turbulence kinetic energy profiles in the near wall region, for flat plate. —— Present work, --- Theory [24], ● Experimental data [25].

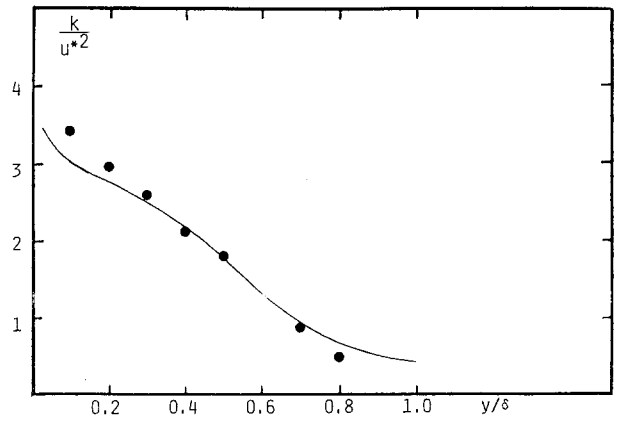

Fig. 3b. Measured and calculated turbulent kinetic energy profile away from the wall, for flat plate. —— Present work, ● Experimental data [26].

models [1, 4, 9] and for two-equation models [3]. Second, a different form for the turbulence length-scale should be used. The following was proposed for (l):

$$l = C_1 y \qquad 0 < y < \frac{C_2}{C_1}\delta$$
$$l_e = C_2\delta \qquad \frac{C_2}{C_1}\delta < y < \delta \tag{16}$$

where C_1, C_2 are constants.

Preliminary numerical computations have been done to determine the sensitivity of the different model constants (A_μ, C_D, C_1, C_2) on the computed friction and heat transfer coefficients. A decision was made to optimize for

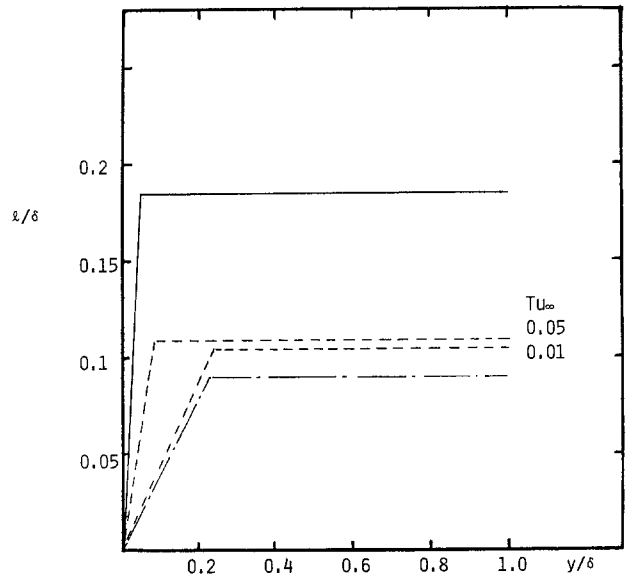

Fig. 4. Turbulence modeling length-scale from different theories. —— Present work, --- Wang [2], –·– Kwon et al. [1].

the two constants C_1 and C_2 only. The optimum values for these constants were obtained by requiring reasonable production of turbulence kinetic energy and reasonable agreement with experimental friction and heat transfer coefficients; the values for C_1 and C_2 were found to be 3.7 and 0.185 respectively.

Figure 4 shows a plot of the turbulence length-scale as proposed by the present study compared with that assumed by Kwon et al. [1] and Wang [2]. It is interesting to notice that Kwon et al. used a constant multiplier B ($B \simeq 2$) with (l) in their formulation for μ_t; this is almost the same factor between the present (l) and what was proposed by Kwon et al.

6. Results and discussion

The above numerical computational scheme has been used to calculate the fluid flow and heat transfer characteristics for a circular cylinder in turbulent cross flow. The computations were performed for a cylinder diameter 10.15 cm; cylinder surface temperature of 278 K and free stream temperature of 280.5 K. The calculations covered a range of Re_D from 30,000 to 250,000 and Tu_∞ up to 7%.

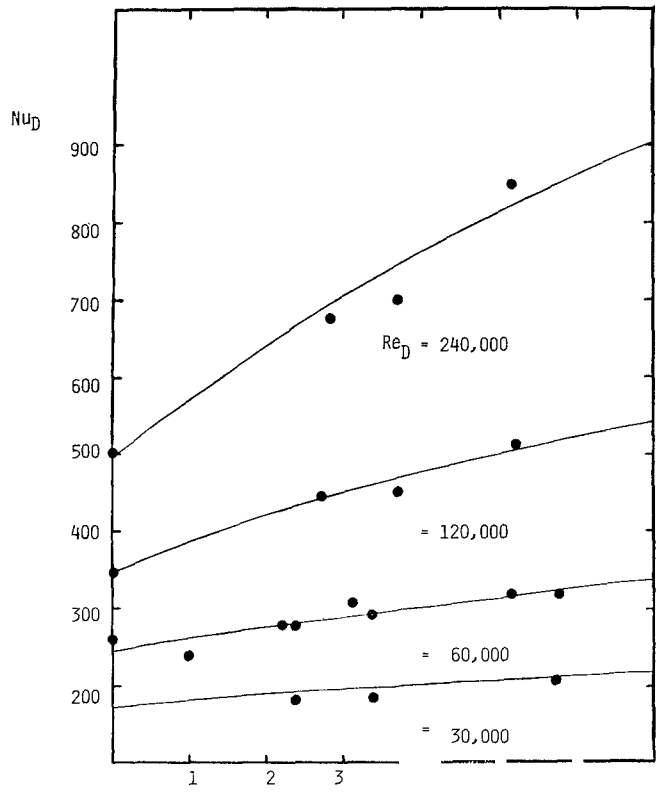

Fig. 5. Comparison between predictions and experimental data near stagnation point Nu_D. —— Present work, ● Experimental data [4].

Figure 5 shows the present model prediction for Nu_D vs. Tu_∞ as compared with the experimental data of Smith and Kuethe [4] for Re_D = 30,000, 60,000, 120,000 and 240,000. The predictions are seen to be in excellent agreement with the data. On Fig. 6, $Nu_D Re_D^{-0.5}$ is plotted vs. $Tu_\infty Re_D^{1/2}$ for different experimental data [4–8] together with the predictions of the present work and other theoretical work [1, 2, 4]. The present model is in good agreement with the data.

On Fig. 7, the wall shear stress (τ_w) normalized with that at zero free stream turbulence intensity ($\tau_{w,0}$) is plotted vs. $Tu_\infty Re_D^{1/2}$ for the present model predictions, and experimental data and predictions of Smith and Kuethe [4]. The present model is in better agreement with the data.

Figure 8 shows the dimensionless streamwise velocity profile (F) plotted against the dimensionless distance (η) for the present work; the experimental data of Kestin and Richardson [27] and the prediction of Wang [2] for Re_D = 250,000 and Tu_∞ = 0.05. The present model is in very good

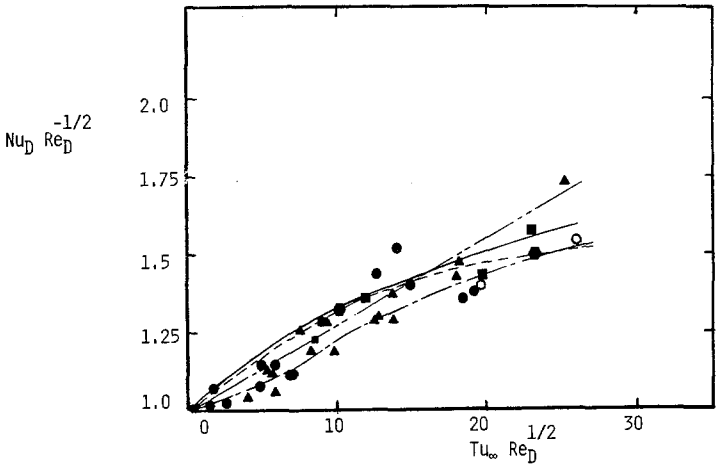

Fig. 6. Stagnation point heat transfer correlations from theories and experiments. Experiment, ▲ Ref. [4], ⬢ Ref. [5], ○ Ref. [6], ● Ref. [7], ■ Ref. [8]. Theory, —— Present work $Re_D = 250{,}000$, – – – Ref. [1], –·– Ref. [2], $Re_D = 250{,}000$, –··– Ref. [4].

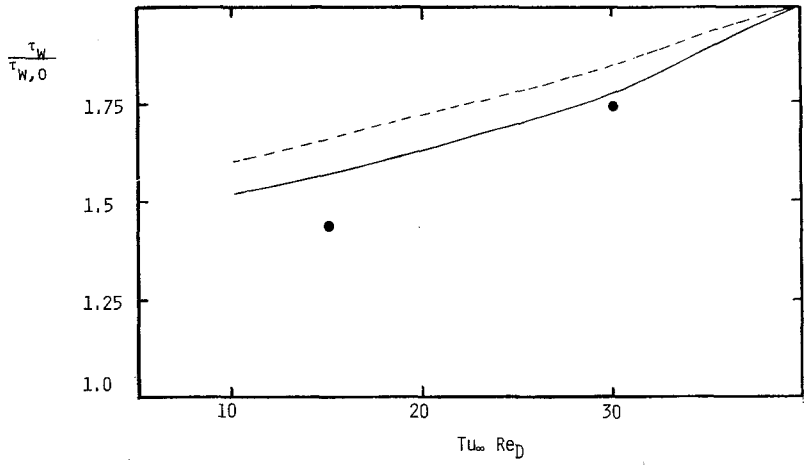

Fig. 7. Stagnation point wall shear stress correlations from theories and experiments. —— Present work, – – – Theory [4], ● Experimental data [4].

agreement with experimental data, while the predictions of Wang is showing, inadequately, a non-zero gradient at far flow field ($y \simeq 8$). On the same plot velocity profile for the laminar flow is shown, the comparison confirms that the turbulent velocity profile has a larger gradient than the laminar one at the surface, while the turbulent boundary layer is thicker, as expected.

Finally, predictions wre made for k/u^{*2} vs. η on Fig. 9 for $Re_D = 60{,}000$, 250,000 and $Tu_\infty = 0.03$, 0.05 and 0.07. The production of the turbulent

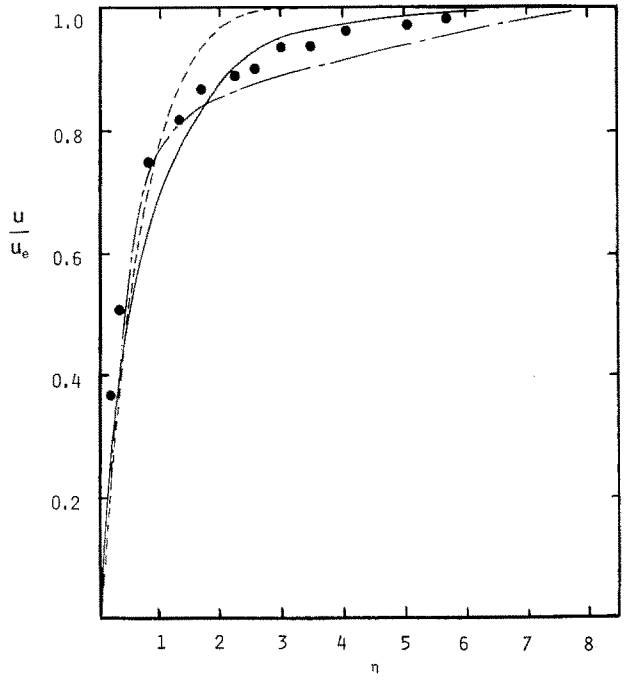

Fig. 8. Mean flow streamwise velocity profiles from theories and experiments, $Re_D = 2.5 \times 10^5$, $Tu_\infty = 0.05$. —— Present work, ---- Laminar flow, -·- Wang [2], ● Experiment [27].

kinetic energy increases as Re_D or Tu_∞ increases. However, the peak value did not change its location (takes place at $\eta \simeq 0.65$). This prediction of the location of maximum (k/u^{*2}) is in close agreement with the data reported by Hijikata et al. [3] but in disagreement with the predictions of Wang [2] showing (k/u^{*2}) max at $\eta \simeq 4.4$. Also, the value of (k/u^{*2}) max predicted with the present model is different from the experimental data of [3] and the prediction of [2]. No firm quantitative conclusion can be drawn at this stage prior to having some experimental data in the near wall region for k.

From the plot on Fig. 9, it is interesting to note that the production of k increases with Tu_∞ at a decreasing rate. This indicates that there is a limiting value for the production of k as Tu_∞ and Re_D increases. Similar assumptions are used in turbine blade heat transfer design [28].

7. Concluding remarks

An implicit finite difference scheme has been described for computing incompressible turbulent flows and heat transfer in the viscinity of the

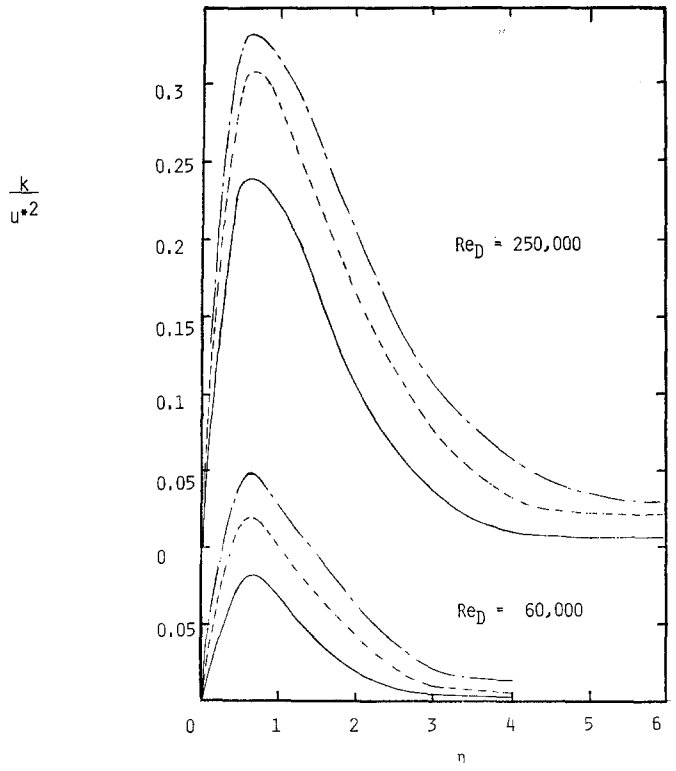

Fig. 9. Predicted profiles of turbulence kinetic energy near the stagnation point. —— $Tu_\infty = 0.03$, – – – $Tu_\infty = 0.05$, –·– $Tu_\infty = 0.07$.

forward stagnation point of a circular cylinder in turbulent cross flow. A one-equation low-Reynolds-number turbulence model has been applied. Using a standard turbulence length-scale, the model predictions were in good agreement with the data for flat plate with zero pressure gradient. On extending the model to the present case of study, it was necessary to exclude the damping function in formulating the turbulent viscosity. Also, a new turbulence length-scale was formulated different than the standard one for flat plate. The new length-scale was twice as much as the standard one in far distance from the wall, and was extended to a closer distance to the wall.

In conclusion, the present study offered a simple turbulence model based on a one-equation low-Reynolds number with a simple turbulence length scale. The model has the same empirical input as used for higher order models and predicted the fluid flow and heat transfer characteristics for the stagnation flow reasonably well.

References

1. O.K. Kwon, E.R. Turner and Y.M. Kou, Prediction of Stagnation Flow Heat Transfer on Turbomachinery Airfoils. *AIAA/SAE/ASME 19th Joint Propulsion Conference*, Seattle, Washington, AIAA-83-1173, June 1983.
2. C.R. Wang, Turbulence and Surface Heat Transfer Near the Stagnation Point of a Circular Cylinder in Turbulent Flow. *ASME Winter Annual Meeting*, New Orleans, Louisiana, December 1984.
3. H. Hijikata, H. Yoshida and Y. Mori, Theoretical and Experimental Study of Turbulence Effects on Heat Transfer Around the Stagnation Point of a Cylinder. *The Seventh International Heat Transfer Conference*, München, Vol. 3 (1982) pp. 165–170.
4. M.C. Smith and A.M. Kuethe, Effects of Turbulence on laminar skin friction and heat transfer. *Physics of Fluids* 9 (12) (1966) 2337–2344.
5. G.M. Zapp, MS Thesis, *Oregon State College* (1950).
6. J.A. Schnautz, Effects of Turbulence Intensity on Mass Transfer from Plates, Cylinders and Spheres in Air Streams. Ph.D. Thesis, *Oregon State College* (1958).
7. G.W. Lowery and R.I. Vachon, The effect of turbulence on heat transfer from heated cylinders. *Int. J. Heat Mass Transfer* 18 (1975) 1229–1242.
8. J. Kestin and R.T. Wood, The influence of turbulence on mass transfer from cylinders. *Journal of Heat Transfer* 93 (1971) 321–326.
9. H. Miyazaki and E.M. Sparrow, Analysis of effects of free-stream turbulence on heat transfer and skin friction. *Journal of Heat Transfer* 99 (1977) 614–619.
10. I.A. Belov, G.F. Gorshkov, V.S. Komarov and V.S. Terpigorev, Effect of jet turbulence on flow in boundary layer near a wall (in Russian). *Zhurnal Prikladoni Mikhaniki Tekhniehoskoi Fiziki* 13 (1972) 77–82.
11. R.M. Traci and D.C. Wilcox, Freestream turbulence effects on stagnation point heat transfer. *AIAA J.* 13 (1975) 890–896.
12. V.C. Patel, W. Rodi and G. Scheuerer, Evaluation of turbulent models for near-wall and low-Reynolds number flows. *Third Symposium on Turbulent Shear Flows*, University of California, Davis, 1981, 1.1–8.
13. M.M. Gibson, An algebraic stress and heat-flux model for turbulent shear flow with streamline curvature. *Int. J. Heat Mass Transfer* 21 (1978) 1609–1617.
14. M.M. Gibson, W.P. Jones and B.A. Younis, Calculation of turbulent boundary layers on curved surfaces. *Physics of Fluids* 24 (3) (1981) 386–395.
15. S.H. El-Tahry, Application of a Reynolds stress model to engine flow calculations, *ASME Winter Annual Meeting*, New Orleans, Louisiana, December 1984.
16. S. Hassid and M. Poreh, A turbulent energy model for flow with drag reduction. *Trans. of the ASME J. Fluids Eng.* 97 (1975) 234–241.
17. M.A.M. El-Hadidy, Applications of low-Reynolds-number turbulence model and wall functions for steady and unsteady heat-transfer computations. Ph.D. Thesis, *Imperial College of Science and Technology*, London (1980).
18. D.A. Anderson, J.C. Tannehill and R.H. Pletcher, *Computational fluid mechanics and heat transfer*. McGraw-Hill (1984) p. 128.
19. R.H. Pletcher, Prediction of incompressible turbulent separating flow. *Journal of Fluids Engineering* 100 (1978) 427–433.
20. J. Nikuradse, Gesetzmassigkeiten der turbuleten Stromung in glatten Rohren. *Forschungsarbeiten Ing. Wesen*, Heft, 356 (1932).
21. I.E. Beckwith and D.M. Bushnell, Detailed description and results of a method for computing mean and fluctuating quantities in turbulent boundary layers. NASA-TN-D-4815 (1968).

22. K. Weighardt and W. Tillman, On the turbulent friction layer for rising pressure. Proceeding of Computation of Turbulent Boundary Layer – 1968, AFOSR-IFP-STANFORD Conference, Vol. II, pp. 98–123.
23. F.M. White, *Viscous Fluid Flow*. McGraw-Hill (1974) p. 341.
24. W.P. Jones and B.E. Launder, The prediction of laminarization with a two-equation model of turbulence. *Int. J. Heat Mass Transfer* 15 (1972) 301–314.
25. H.P. Kerplin and H. Eckelmann, Behavior of three fluctuating velocity components in the wall region of a turbulent flow. *Physics of Fluids* 22 (1979) 1233–1239.
26. J.O. Hinze, *Turbulence*, 2nd edn. New York: McGraw-Hill (1975) p. 642.
27. J. Kestin and P.D. Richardson, The effects of free-stream turbulence and of sound upon heat transfer, ARL-69-0062, Wright-Patterson AFB, Dayton, Ohio (1969).
28. A.J. Glassman, Turbine design and application, NASA SPL-290, Vol. 3 (1975).